Bioluminescence imaging of human embryonic stem cells transplanted in vivo in murine and chick models.

Helen Priddle[1*], Anna Grabowska[2*‡], Teresa Morris[2], Philip A Clarke[2], Andrew J McKenzie[2], Virginie Sottile[3], Chris Denning[3], Lorraine Young[1,3] Sue Watson[2].

[1] School of Human Development, D Floor, East Block, University of Nottingham, Queens Medical Centre, Nottingham, UK

[2] Division of Pre-Clinical Oncology, University of Nottingham, Nottingham, UK

[3] Wolfson Centre for Stem cells, Tissue Engineering and Modelling (STEM), Centre for Biomolecular Sciences, University of Nottingham, Nottingham, NG7 2RD, UK

*** Joint first authors**

Running Title: Bioluminescent imaging of human embryonic stem cells

Abbreviations: ESC- Embryonic Stem Cell; hESC- Human Embryonic Stem Cell

[‡] Corresponding author:

Dr. A. Grabowska

Division of Pre-Clinical Oncology

University of Nottingham

West Block, D floor,

Queen's Medical Centre

Nottingham, NG7 2UH

United Kingdom

ABSTRACT

Research into the behaviour, efficacy and biosafety of stem cells with a view to clinical transplantation requires the development of non-invasive methods for *in vivo* imaging of cells transplanted into animal models. This is particularly relevant for human embryonic stem cells (hESCs), since transplantation of undifferentiated hESCs leads to tumor formation. The present study aimed to monitor hESCs in real time when injected *in vivo*. hESCs were stably transfected to express luciferase, and luciferase expression was clearly detected in the undifferentiated and differentiated state. When transfected hESCs were injected into chick embryos, bioluminescence could be detected both *ex* and *in ovo*. In the SCID mouse model, undifferentiated hESCs were detectable after injection either into the muscle layer of the peritoneum or the kidney capsule. Tumours became detectable between days 10-30, with approximately a 3 log increase in the luminescence signal by day 75. The growth phase occurred earlier in the kidney capsule and then reached a plateau, whilst tumours in the peritoneal wall grew steadily throughout the period analysed. These results show the widespread utility of bioluminescent *in vivo* imaging of hESCs in a variety of model systems for pre-clinical research into regenerative medicine and cancer biology.

INTRODUCTION

A classical measure of the pluripotency of embryonic stem cells (ESC) is the ability to form derivatives of the three primitive germ layers; endoderm, ectoderm and mesoderm. This can be assessed *in vitro* through the formation of embryoid bodies, but a wider range of cell types are typically observed when ESCs are transplanted into immunocompromised mice, where they form teratomas (Cooke *et al.*, 2006). For example, insulin was not detected in embryoid bodies from hESCs derived from cells transfected with the *Pdx1* promoter in order to drive *in vitro* differentiation of pancreatic cell types; however, it was detected when the cells were differentiated *in vivo* in teratomas (Lavon *et al.*, 2006). This illustrates the current inadequacy of many *in vitro* differentiation procedures to produce the full range of desired stem cell types *in vitro*, where the complex signals of an *in vivo* niche are not recapitulated. Teratomas thus represent a unique *in vivo* model to study aspects of early human tissue development (Cooke *et al.*, 2006).

Unintentional teratoma formation is also of great concern when ESC derivatives are transplanted, potentially either through the co-transplantation of undifferentiated cells or through dedifferentiation. Studies of teratoma formation from ESC-derived transplants have resulted in highly variable outcomes (Shibata *et al.*, 2006). Allogeneic transplantation of Cynomolgus monkey ESC-derived putative haematopoeitic precursors resulted in teratoma formation in newborns, whereas transplantation of the same cells in immunodeficient mice or fetal sheep did not (Sasaki *et al.*, 2005) and the period of *in vitro* differentiation prior to transplantation was found to influence whether or not teratomas were formed. It is unclear whether this difference in outcome is influenced by immunological status (both in terms of immune-competence and crossing of species barriers) or environment (in terms of site of injection and developmental stage), illustrating the need for much greater understanding of the conditions required for teratoma growth post-transplantation in order to be able to extrapolate confidently to a clinical setting. We aim to develop methodology enabling real-time tracking of hESCs and teratoma formation *in vivo*.

Currently, the formation of teratomas is detected in SCID mice either by sacrificing mice at a pre-determined timepoint or when the tumours reach an advanced stage and palpable size. A recent report has also described differences in the kinetics of teratoma growth and in morphology of the composite cell types, depending on the site of injection of the pluripotent, human embryonal carcinoma cells studied (Cao *et al.*, 2006). *In vivo* imaging using an MRI approach has recently demonstrated the possibility of imaging hESCs injected into the hearts of cyclosporine-treated rats at 24h and 5 days post-surgery (Tallheden *et al.*, 2006). In this model, signs of immune rejection of the cells were evident at five days. Moreover, the cell division-related reduction in the signal from the small particles of iron oxide introduced into pre-transplant hESCs is a major barrier to long-term *in vivo* imaging by this method. Transfection of the estrogen receptor ligand binding domain into mouse ESC has allowed *in vivo* positron emission tomography to be used to monitor transplantation into nude mice and subsequent teratoma formation (Takamatsu *et al.*, 2005); however, this approach requires access to radiolabelling, cyclotron and PET imaging technology, which are not readily available to most researchers.

In the present study, we investigated bioluminescence imaging ,using the luminescent substrate, D-luciferin. This technique is capable of detecting cells stably expressing firefly luciferase over long periods *in vivo* (Burgos *et al.*, 2003; Edinger *et al.*, 2003; Wang *et al.*, 2003). In addition to the increased sensitivity of detection of luciferase relative to GFP (Gisela Caceres, 2003), luciferase was shown to be non-immunogenic in rats, whereas GFP-expressing skin grafts were rejected in less than 10 days (Hakamata *et al.*, 2006). Bioluminescence imaging has been used recently for the relatively short–term (1-2 week) live imaging of an embryonic rat cardiomyoblast cell line (Krishnan *et al.*, 2006) and of human cord blood derived mesenchymal stem cells in rat myocardium over 8 days. In the current study we examined the utility of this method for hESC bioluminescent imaging in mouse and chick models, and followed teratoma formation in SCID mice over a 75 day

period, after injection either into the peritoneal muscle wall (Watson *et al.*, 1999) or the kidney capsule.

In addition to the study of teratoma formation from hESCs, the ability to track hESC derivatives after transplantation to observe their migration, survival, proliferation and further differentiation is essential to our understanding of the biology and clinical utility of these cells (Krishnan *et al.*, 2006). The development of a range of transplantation models is of increasing importance for both cancer and stem cell research, as the mouse model is not always the most appropriate (Sasaki *et al.*, 2005). Cell transplantation into chick embryos offers a high throughput allowing the screening of many cell lines and treatments in a short period of time. Because of its ease of use and inherent immunotolerance, it is a well-established model to analyse the growth and potential of injected xenogeneic cell lines (Tsuchiya *et al.*, 1994; Kobayashi *et al.*, 1998; Cretu *et al.*, 2005), including hESCs (Goldstein *et al.*, 2002).

The aims of the current study were to (i) evaluate the possibility of expressing luciferase in hESCs; (ii) investigate multiple models and sites for transplantation and bioluminescent tracking *in vivo*; and (iii) use real-time, *in vivo* bioluminescent imaging to monitor the growth of teratomas in both the peritoneal cavity and kidney capsule over a period of 75 days.

METHODS AND MATERIALS

Unless otherwise stated, reagents were supplied by Invitrogen.

Cell Culture

BGN01 hESCs (Mitalipova *et al.*, 2003) were obtained from BresaGen (Athens, Georgia) and were cultured as described previously. This feeder-free system uses Matrigel matrix (BD Biosciences) and mouse embryonic fibroblast (MEF)-conditioned medium, changed daily. The medium used for conditioning contained 80% DMEM-F12, 20% KnockOut Serum Replacement, 1X MEM Non-essential amino acids (MEM-NEAA), 2 mM L-Glutamine, 100 μM 2-mercaptoethanol (Sigma) and 4ng/ml basic FGF (Sigma).

The human prostate cancer cell line, PC3M-luc (Xenogen, USA) was cultured in RPMI 1640 culture medium (Gibco, Paisley, UK) containing 10% (v/v) heat inactivated foetal bovine serum (FBS, Sigma, Poole, UK). Cells were passaged by treatment with 0.05% Trypsin/EDTA and were incubated at 37°C in 5% CO_2 and humidified conditions.

Transfection of hESCs

A vector for stable and constitutive expression of luciferase in eukaryotic cells was constructed based on the pCAGGFPIP vector (kind gift of Ian Chambers, University of Edinburgh). This comprises a chicken β-actin/CMV enhancer promoter upstream of EGFP coding sequence and an independent ribosome entry site (IRES) which enables translation of a downstream puromycin resistance coding sequence. The EGFP coding sequence was replaced with the luciferase coding sequence of pGEM-Luc (Promega) to form pCAGLucIP. Stable transfection of hESCs with the vector was as described in (Priddle, 2003). In brief, pCAGLucIP vector was linearised and mixed with $1x10^6$ BGN01 hESCs , pre-swollen in Hypo-osmolar Electroporation Buffer (Eppendorf) in a 0.4 cm gap Electroporation cuvette (Eppendorf). A pulse of 440 V for 100 μs was applied at room temperature using a Multiporator (Eppendorf) and the mix was incubated at room temperature for 10 minutes.

The cells were plated onto a 9 cm Matrigel coated dish in a maximal volume of MEF-conditioned medium and cultured for 48 hours before application of 300ng/ml Puromycin (Sigma) until hESC colonies became visible by eye. Colonies of 'hESC-Luc' cells were picked and individually expanded in MEF conditioned medium using Matrigel coated wells.

Assay for Luciferase Expression in Cells

Undifferentiated hESCs and PC3M-lucs were treated with 0.05% Trypsin/EDTA to generate a single cell suspension. *In vitro* differentiated, hESC-derived embryoid bodies were disaggregated by treatment with 0.4 U/ml Collagenase B (Roche) for 2 hours at 37ºC followed by a 10 minute incubation in Cell Dissociation Buffer. Cells were counted, resuspended in PBS (without Ca^{2+} and Mg^{2+}) and a defined number of cells aliquoted into a white microtitre plate (Nalge Nunc) in a volume of 100 µl. An equal volume of Steady-Glo Luciferase Assay solution (Promega) was added, mixed and the cells incubated for 5 minutes at room temperature before detection in a MicroLumi XS luminometer (Harta) or using the IVIS® X100 biophotonic imaging system (Xenogen).

Differentiation of hESCs

hESCs were transferred to a 9cm dish of inactivated MEF feeders (treated with 10 µg/ml mitomycin C (Sigma) for 2.5 hours and plated at $6x10^4$ cells/cm^2) to improve embryoid body formation (Denning *et al.*, 2006). Once the cells reached confluence they were treated with 1 mg/ml Collagenase IV (Invitrogen) for 15 minutes at 37ºC and were scraped to liberate cell clumps. These were suspended in MEF-conditioned medium in plastic Petri dishes to promote aggregation. Embryoid bodies were cultured in suspension in conditioned medium for 3 days and were then plated on gelatinised 6 cm tissue culture dishes in differentiation medium (80% DMEM, 20% FBS, 1X MEM-NEAA, 2mM L-Glutamine, 100µM 2-mercaptoethanol) for 14 days to allow undirected differentiation.

Preparation of hESC-Luc cells for *in vivo* injection

hESC-Luc cells were cultured on Matrigel in MEF-conditioned medium and were harvested by incubation with 0.05% trypsin/EDTA. Cells were resuspended in PBS (without Ca^{2+} and Mg^{2+}) for transplantation.

Chick Embryo Husbandry and Cell Injection

White Leghorn fertile eggs purchased from Henry Stewart & Co. (Louth, UK) were incubated in a humidified incubator with periodical agitation for 2.3-4.5days (HH stage 16-25). The hESC cell suspension, prepared in PBS, was injected into chick embryos either *in ovo* or after dissection as specified. For bioluminescence analyses carried out *in ovo*, 2μg/μl D-luciferin substrate were added to the cell suspension. For analyses performed *ex ovo*, dissected embryos were incubated for 10min in a solution containing 2μg/μl D-luciferin substrate and transferred to a Petri dish before measurements with the IVIS® X100 imaging system.

Mouse Husbandry and Cell Injection

This work was carried out under Home Office Project Licence 40/2323 (Watson). All surgery was carried out using aseptic technique in a Class II Biosafety cabinet. For injection into the peritoneal muscle wall, the mouse was anaesthetised (Hypnorm, Roche/Hypnovel, Janssen), and a small incision made in the left flank. 50μl of cell inoculum was injected into the peritoneal muscle wall and the skin is then closed with surgical clips. For injection into the kidney capsule, the mouse was anaesthetised (Hypnorm, Roche/Hypnovel, Janssen) and a pre-operative dose of Rimadyl (Pfizer Animal Health) administered subcutaneously. A small incision was made on the left flank of the animal through the skin and the peritoneal wall. The left kidney was gently exteriorized, 20μl of cell suspension injected into the kidney capsule and the kidney then gently replaced within the peritoneal cavity. The peritoneal muscle wall was sutured and the skin closed with surgical clips. The mice were closely

monitored throughout the study by an experienced animal technician and their bodyweight measured weekly.

Imaging of hESC-Luc cells – Living Image Software

Mice were anaesthetized as above and, 15 minutes prior to imaging, D-Luciferin substrate was injected into the peritoneal cavity (60 mg/kg in sterile PBS). Luminescence emitted by cells was captured using the IVIS® X100 imaging system (Caliper Life Sciences) and quantified with Living Image/Igor Pro Software (Caliper Life Sciences). Areas of luminescence were identified as Regions of Interest (ROIs) and quantified as photons emitted. Mice were also photographed under brightfield conditions to allow localization of signal.

The *in vivo* measurements were collated over the duration of the experiment so that cell growth and distribution could be accurately monitored in individual mice. Photographic images of the subjects were overlaid with a pictorial representation of the intensity of photons emitted, to represent the localization of the signal and the differences of light intensity detected (from blue = low light levels to red = high levels).

Histology of teratomas

After 75 days, any growths formed were removed and fixed in 4% paraformaldehyde. Fixed tissues were dehydrated and embedded in paraffin wax using a Shandon Excelsior (Thermo Electron Corp.) automated tissue processor. 5µm sections were cut using a microtome and were stained with haematoxylin and eosin by standard histological protocols to reveal histological detail.

RESULTS

Establishing luciferase-expressing hESCs and luciferase imaging *ex vivo*

After stable transfection of BGN01 hESCs with the luciferase expression vector pCAGLucIP, eight colonies were clonally expanded (hESC-Luc1 to hESC-Luc8). Upon initial screening for luciferase expression, hESC-Luc7 and hESC-Luc8 were found to have the greatest expression levels (data not shown) and were utilised for further studies.

Using the IVIS® X100 system, the luminescence of $1x10^3$, $1x10^4$ and $1x10^5$ hESC-Luc7 and hESC-Luc8 was compared with PC3-luciferase-transfected cells (a human prostate cancer cell line) *in vitro* (Figure 1). The luminescence of hESC clones was comparable to that of the PC3 cell line and correlated with cell number. hESC-Luc7 and hESC-Luc8 clones continued to express luciferase over 25 passages / 11 weeks.

Luciferase expression is maintained in differentiated hESCs

hESC-Luc7 and hESC-Luc8 were transferred from feeder-free culture to culture in unconditioned medium on inactivated MEF feeders in order to promote embryoid body formation (Denning *et al.*, 2006). Cells were harvested and suspended in uncoated 9cm plastic Petri dishes in conditioned medium for 3 days to form induce formation of embryoid bodies. These were cultured in serum-based medium for 2 weeks to allow undirected differentiation. The tissues formed were disaggregated and $5x10^4$ of differentiated (or undifferentiated control cells were assayed for luciferase expression using the MicroLumi XS luminometer. As shown in Figure 2, luciferase expression was not only maintained upon differentiation but was increased in both clones. Since both clones had similar luminescence in the undifferentiated state and clone 8 had higher luminescence following differentiation, hESC-luc8 was selected for the remainder of the study.

Luciferase positive cells imaged in chick embryos *ex ovo* and *in ovo*

In order to test whether hESC-Luc cells could be detected following transplantation *in vivo*, the chick embryo model was initially used. Increasing numbers of h300ESC-Luc cells were injected into chick embryos and the resulting signal analysed with the IVIS® X100 system. In HH stage 16 embryos analysed *ex ovo*, luciferase activity was clearly detected in embryos injected with 10^4 cells and 10^5 cells (Fig. 3A). The possibility that luminescence measurements could be analysed *in ovo* was also investigated. Despite the presence of the shell and egg yolk mass, embryos injected with both 10^4 and 10^5 cells generated marked bioluminescent signals quantifiable *in ovo* (Fig. 3C-E). However, no significant luminescence value could be detected *in ovo* for embryos which had been injected with 10^3 cells (Fig. 3B).

Monitoring development of teratomas *in vivo* in SCID mice

In order to investigate the feasibility of imaging the hESC-luc clones *in vivo* in a mouse model the limits of detection for hESC-luc cells was estabilshed using $1x10^4$, $1x10^5$, or $1x10^6$ cells; compared to a positive control of $1x10^5$ PC3M-luc cells. Cells were injected into the peritoneal muscle wall or kidney capsule of terminally anaesthetised mice. Following intra-peritoneal administration of luciferin, the mice were imaged using the IVIS® X100 system. Both $1x10^5$ and $1x10^6$ hESC-luc7 cells were clearly visible (ROI of $4.2x10^5$ and $3.3x10^6$ respectively vs $5.0x10^6$ for the PC3M-lucs; data not shown). The sensitivity of detection was lower for cells injected into the kidney capsule (ROI of $0.7x10^5$ and $3.7x10^5$ respectively vs $1.1x10^6$ for the PC3M-luc cells; data not shown), possibly due to the greater tissue depth which may lead to loss of signal through absorption. However, these data probably underestimate the sensitivity of detection, as these measurements were carried out in animals after sacrifice, and thus the substrate may not reach the kidney capsule as effectively as in a live recipient.

hESC-luc cells were next used to investigate the possibility of monitoring teratoma formation in real time. Two inoculation sites were used, peritoneal muscle wall (Figure 4A) and kidney capsule (Figure 4B), and the mice were imaged at 3-6 day intervals. At both sites, 3 of the 5

mice developed luminescent areas that could be imaged using the IVIS® X100 and which increased with time. The signals from the tumours that formed in the peritoneal wall were variable in the initial phase between day 10-30, and then grew steadily over a period of 30-70 days. Approximately a 3-log increase in the luminescence signal was detected over the 75 day experimental period with all three tumours having a similar growth profile.

In the kidney capsule, two of the tumours were visible by day 20, and grew steadily, reaching a plateau at day 40. The third tumour was only detectable from day 30 but in all tumours that developed a 3-log increase in the luminescence signal was achieved by the end of the experiment (d75).

At the end of the experiment the tissues that developed were removed and subjected to histological analysis. The teratomas formed were mostly cystic, with cyst walls composed of layers of dense extracellular matrix (Figure 5a). Some solid teratoma tissue was found, which had well-differentiated tissues, such as smooth muscle (Figure 5b), gut-like secretory epithelium (Figure 5c) and cartilage (Figure 5d)

DISCUSSION

This study confirmed that stable transfection of hESCs with a firefly luciferase reporter had no apparent detrimental effect on hESC viability, proliferation or differentiation potential, as previously reported for mouse ESCs (Cao *et al.*, 2006).

Since viral promoters are particularly prone to such silencing mechanisms in both mouse and human ESCs, the current study investigated the utility of the chicken B actin promoter (Fregien and Davidson, 1986), which has been reported to offer robust transgene expression in ES cell lines (Xia et al. 2007, Costa et al. 2005). Previous studies in somatic cells have used a cytomegalovirus (CMV) promoter to drive luciferase expression (Krishnan *et al.*, 2006) but observed progressive decrease of luciferase reporter activity over time. Rescue of activity with the DNA methylation inhibitor, 5-azacytidine, indicated that the CMV promoter was prone to epigenetic silencing (Krishnan *et al.*, 2006).

In vitro, there was higher luciferase activity in differentiated cells, which may be explained by a greater activity of the CAG promoter and/or a larger cytoplasmic volume in differentiated cells, or a different passage number in the undifferentiated cells leading to increased silencing (the undifferentiated cells measured here were 7 passages higher than the differentiated cells).

The study demonstrated that this bioluminescent technique allows short term *in vivo* imaging in the chick embryo model, which is increasingly used to assess the proliferation, differentiation and migration capacity of rodent and human stem cells (Demeter *et al.*, 2004; Fernandes *et al.*, 2004; Pochampally *et al.*, 2004). The chick embryo model has been widely used for the analysis of tumorigenicity using multiple cancer cell lines (Knighton *et al.*, 1977; Chambers *et al.*, 1982; Luyten *et al.*, 1993). Interestingly, the limit for *in ovo* detection described in our study is compatible with the number of cells ($2x10^4$ to 10^5 cells) routinely injected for tumourigenic assays [Demeter et al. (2004), Cretu et al. (2005)]. The throughput of the chick embryo model for xenogeneic transplantation could thus be further

enhanced if combined to this novel graft monitoring techniques to assess injected embryos displaying the higher number of engrafted cells.

Our study also demonstrates that using this approach it is possible to monitor the growth of teratomas formed from hESCs in SCID mice over a period of 75 days, as the hESCs retained luciferase expression *in vivo* over this period. In initial studies with cells injected into the peritoneal cavity and kidney capsule of terminated mice, we were able to detect smaller numbers of cells ($1x10^5$) than in a recent study using the same system in rats which reported that $1x10^6$ human cord blood-derived mesenchymal stem cells delivered intramyocardially could be successfully imaged (Min *et al.*, 2006). This may be a result of higher luciferase expression in the transfected hESC-luc cells used in this study.

Following injection of hESC-luc into live mice to monitor teratoma formation, cells were only detected in the injection site, but small numbers of migrating cells would be below the sensitivity limits of detection for the assay. Iron particle labeling of ES cells might enable better fine-resolution tracking of cells *in vivo*, but this approach is not applicable for longer term studies as the particles are rapidly diluted by cell division and rendered undetectable (Li *et al.*, 2008). Quantum dot (nanocrystals which emit light upon excitation) imaging provides an opportunity for photobleaching-resistant multiplex imaging. Importantly, Quantum Dots have been shown to be inert in mouse ESCs. However, the signal is undetectable 14 days after transplantation of the labeled ESCs *in vivo*, and so like iron particles, gives a limited tracking period compared to the approach described here (Lin *et al.*, 2007).

To date, the long-term follow-up of hESC derivatives transplanted into mouse models has been limited to end-point measures when the animals are sacrificed (Tian *et al.*, 2006). Teratoma formation after cardiac delivery of mouse ESCs has previously been followed over 4 weeks (Cao *et al.*, 2006), with an increase in bioluminescence signal observed over time as in the current study. This is consistent not only with sustained expression of exogenous luciferase in hESC cells post-transplantation, but increased proliferation in the host. The

extension of the current study to a period of 75 days illustrates the long-term utility of this approach required for hESC studies. As described previously for liver versus subcutaneous implants (Cooke *et al.*, 2006), we observed different growth kinetics of teratomas formed in the kidney and peritoneal cavity, confirming the ability of differing environmental cues to influence stem cell behaviour.

The availability of whole mice and rats expressing luciferase provides the potential to also compare the behaviour of a variety of fetal and adult stem cell types via bioluminescence imaging in a range of transplantation sites. Similar bioluminescence imaging of mouse neural stem/ progenitor cells enabled their detection in spinal cord-injured mice for approximately 10 months. Long-term persistence and biodistribution of multipotent adult progenitor cells has also been described where these cells have been infused intravenously (Tolar *et al.*, 2006).

Whether transplantation of differentiated ESCs leads to teratoma formation from residual undifferentiated cells, from more advanced progenitor cell types or from dedifferentiated cells remains the subject of debate. The removal of SSEA-4 (a marker of pluripotency) positive cells from *in vitro* differentiated haematopoeitic precursor populations prior to allogeneic transplantation of Cynomolgus monkey obviated the formation of teratomas, suggesting that undifferentiated cells are the cause. Consistent with this, *in vitro* differentiation of hESC dopaminergic neurons for 16 days and subsequent transplantation resulted in teratoma formation in rat brains post-transplantation, whereas those predifferentiated *in vitro* for 23 days did not (Brederlau *et al.*, 2006). In our laboratory, OCT-4 expression in hESC-derived embryoid bodies is undetectable by immunohistochemistry or PCR after 16 days of differentiation (Burridge, Thymi, Priddle & Young, unpublished data), suggesting that progenitors as well as undifferentiated cells can contribute to teratoma formation.

In conclusion, the use of bioluminescent imaging of luciferase expressing hESCs provides an effective method facilitating the non-invasive, long-term, real time imaging of hESCs

transplanted *in vivo.* The ability to monitor regularly without adverse effects on the mouse hosts represents significant progress towards the reduction, refinement and replacement goals of National Centre for the Replacement, Refinement and Reduction of Animals in Research and international animal welfare objectives. This technology will be invaluable for the development of stem cell-based approaches for therapy, by providing an *in vivo* readout alowing (i) testing of methods to overcome the immune barrier in stem cell therapies (Min *et al.*, 2006); (ii) optimization of protocols for delivery of functional tissues (for example, Brederlau et al., 2006) (iii) monitoring of cell dissemination after delivery; and (iv) validation of strategies to prevent teratoma formation (Hewitt *et al.*, 2007). Such modeling experiments *in vivo* are essential to ensure the effective and safe translation of ESC-based stem cell strategies towards clinical applications.

Acknowledgements:

VS is indebted to the Anne McLaren fellowship scheme (University of Nottingham) and to the Alzheimer's Society for their support, past and present.

REFERENCES

Brederlau, A., A. S. Correia, S. V. Anisimov, M. Elmi, G. Paul, L. Roybon, A. Morizane, F. Bergquist, I. Riebe, U. Nannmark, M. Carta, E. Hanse, J. Takahashi, Y. Sasai, K. Funa, P. Brundin, P. S. Eriksson and J. Y. Li (2006). Transplantation of human embryonic stem cell-derived cells to a rat model of Parkinson's disease: effect of in vitro differentiation on graft survival and teratoma formation. Stem Cells. 24, 1433-40.

Burgos, J. S., M. Rosol, R. A. Moats, V. Khankaldyyan, D. B. Kohn, M. D. Nelson, Jr. and W. E. Laug (2003). Time course of bioluminescent signal in orthotopic and heterotopic brain tumors in nude mice. Biotechniques. 34, 1184-8.

Cao, F., S. Lin, X. Xie, P. Ray, M. Patel, X. Zhang, M. Drukker, S. J. Dylla, A. J. Connolly, X. Chen, I. L. Weissman, S. S. Gambhir and J. C. Wu (2006). In vivo visualization of embryonic stem cell survival, proliferation, and migration after cardiac delivery. Circulation. 113, 1005-14.

Chambers, A. F., R. Shafir and V. Ling (1982). A model system for studying metastasis using the embryonic chick. Cancer Res. 42, 4018-25.

Cooke, M. J., M. Stojkovic and S. A. Przyborski (2006). Growth of teratomas derived from human pluripotent stem cells is influenced by the graft site. Stem Cells Dev. 15, 254-9.

Cretu, A., J. S. Fotos, B. W. Little and D. S. Galileo (2005). Human and rat glioma growth, invasion, and vascularization in a novel chick embryo brain tumor model. Clin Exp Metastasis. 22, 225-36.

Demeter, K., B. Herberth, E. Duda, A. Domonkos, T. Jaffredo, J. P. Herman and E. Madarasz (2004). Fate of cloned embryonic neuroectodermal cells implanted into the adult, newborn and embryonic forebrain. Exp Neurol. 188, 254-67.

Denning, C., C. Allegrucci, H. Priddle, M. D. Barbadillo-Munoz, D. Anderson, T. Self, N. M. Smith, C. T. Parkin and L. E. Young (2006). Common culture conditions for maintenance and cardiomyocyte differentiation of the human embryonic stem cell lines, BG01 and HUES-7. Int J Dev Biol. 50, 27-37.

Edinger, M., P. Hoffmann, C. H. Contag and R. S. Negrin (2003). Evaluation of effector cell fate and function by in vivo bioluminescence imaging. Methods. 31, 172-9.

Fernandes, K. J., I. A. McKenzie, P. Mill, K. M. Smith, M. Akhavan, F. Barnabe-Heider, J. Biernaskie, A. Junek, N. R. Kobayashi, J. G. Toma, D. R. Kaplan, P. A. Labosky, V. Rafuse, C. C. Hui and F. D. Miller (2004). A dermal niche for multipotent adult skin-derived precursor cells. Nat Cell Biol. 6, 1082-93.

Fregien, N. and N. Davidson (1986). Activating elements in the promoter region of the chicken beta-actin gene. Gene. 48, 1-11.

Gisela Caceres, X. Y. Z. J.-a. J. R. Z. A. A. P. A. (2003). Imaging of luciferase and GFP-transfected human tumours in nude mice. Luminescence. 18, 218-223.

Goldstein, R. S., M. Drukker, B. E. Reubinoff and N. Benvenisty (2002). Integration and differentiation of human embryonic stem cells transplanted to the chick embryo. Dev Dyn. 225, 80-6.

Hakamata, Y., T. Murakami and E. Kobayashi (2006). "Firefly rats" as an organ/cellular source for long-term in vivo bioluminescent imaging. Transplantation. 81, 1179-84.

Hewitt, Z., H. Priddle, A. J. Thomson, D. Wojtacha and J. McWhir (2007). Ablation of undifferentiated human embryonic stem cells: exploiting innate immunity against the Gal alpha1-3Galbeta1-4GlcNAc-R (alpha-Gal) epitope. Stem Cells. 25, 10-8.

Knighton, D., D. Ausprunk, D. Tapper and J. Folkman (1977). Avascular and vascular phases of tumour growth in the chick embryo. Br J Cancer. 35, 347-56.

Kobayashi, T., K. Koshida, Y. Endo, T. Imao, T. Uchibayashi, T. Sasaki and M. Namiki (1998). A chick embryo model for metastatic human prostate cancer. Eur Urol. 34, 154-60.

Krishnan, M., J. M. Park, F. Cao, D. Wang, R. Paulmurugan, J. R. Tseng, M. L. Gonzalgo, S. S. Gambhir and J. C. Wu (2006). Effects of epigenetic modulation on reporter gene expression: implications for stem cell imaging. FASEB J. 20, 106-8.

Li, Z., Y. Suzuki, M. Huang, F. Cao, X. Xie, A. J. Connolly, P. C. Yang and J. C. Wu (2008). Comparison of reporter gene and iron particle labeling for tracking fate of human embryonic stem cells and differentiated endothelial cells in living subjects. Stem Cells. 26, 864-73.

Lin, S., X. Xie, M. R. Patel, Y. H. Yang, Z. Li, F. Cao, O. Gheysens, Y. Zhang, S. S. Gambhir, J. H. Rao and J. C. Wu (2007). Quantum dot imaging for embryonic stem cells. BMC Biotechnol. 7, 67.

Luyten, G. P., C. M. Mooy, P. T. De Jong, A. T. Hoogeveen and T. M. Luider (1993). A chicken embryo model to study the growth of human uveal melanoma. Biochem Biophys Res Commun. 192, 22-9.

Min, J. J., Y. Ahn, S. Moon, Y. S. Kim, J. E. Park, S. M. Kim, U. N. Le, J. C. Wu, S. Y. Joo, M. H. Hong, D. H. Yang, M. H. Jeong, C. H. Song, Y. H. Jeong, K. Y. Yoo, K. S. Kang and H. S. Bom (2006). In vivo bioluminescence imaging of cord blood derived mesenchymal stem cell transplantation into rat myocardium. Ann Nucl Med. 20, 165-70.

Mitalipova, M., J. Calhoun, S. Shin, D. Wininger, T. Schulz, S. Noggle, A. Venable, I. Lyons, A. Robins and S. Stice (2003). Human embryonic stem cell lines derived from discarded embryos. Stem Cells. 21, 521-6.

Pochampally, R. R., B. T. Neville, E. J. Schwarz, M. M. Li and D. J. Prockop (2004). Rat adult stem cells (marrow stromal cells) engraft and differentiate in chick embryos without evidence of cell fusion. Proc Natl Acad Sci U S A. 101, 9282-5.

Priddle, H. (2003). Transfection of human ES cells. In Gene Targeting and Embryonic Stem Cells. J. McWhir and A. Thomson, eds. (BIOS Scientific Publishers Ltd., Abingdon, UK).

Sasaki, K., Y. Nagao, Y. Kitano, H. Hasegawa, H. Shibata, M. Takatoku, S. Hayashi, K. Ozawa and Y. Hanazono (2005). Hematopoietic microchimerism in sheep after in utero transplantation of cultured cynomolgus embryonic stem cells. Transplantation. 79, 32-7.

Shibata, H., N. Ageyama, Y. Tanaka, Y. Kishi, K. Sasaki, S. Nakamura, S. Muramatsu, S. Hayashi, Y. Kitano, K. Terao and Y. Hanazono (2006). Improved safety of hematopoietic transplantation with monkey embryonic stem cells in the allogeneic setting. Stem Cells. 24, 1450-7.

Takamatsu, S., T. Furukawa, T. Mori, Y. Yonekura and Y. Fujibayashi (2005). Noninvasive imaging of transplanted living functional cells transfected with a reporter estrogen receptor gene. Nuclear Medicine and Biology. 32, 821-829.

Tallheden, T., U. Nannmark, M. Lorentzon, O. Rakotonirainy, B. Soussi, F. Waagstein, A. Jeppsson, E. Sjogren-Jansson, A. Lindahl and E. Omerovic (2006). In vivo MR imaging of magnetically labeled human embryonic stem cells. Life Sci. 79, 999-1006.

Tian, X., P. S. Woll, J. K. Morris, J. L. Linehan and D. S. Kaufman (2006). Hematopoietic engraftment of human embryonic stem cell-derived cells is regulated by recipient innate immunity. Stem Cells. 24, 1370-80.

Tolar, J., J. O'Shaughnessy M, A. Panoskaltsis-Mortari, R. T. McElmurry, S. Bell, M. Riddle, R. S. McIvor, S. R. Yant, M. A. Kay, D. Krause, C. M. Verfaillie and B. R. Blazar (2006). Host factors that impact the biodistribution and persistence of multipotent adult progenitor cells. Blood. 107, 4182-8.

Tsuchiya, Y., Y. Endo, H. Sato, Y. Okada, M. Mai, T. Sasaki and M. Seiki (1994). Expression of type-IV collagenases in human tumor cell lines that can form liver colonies in chick embryos. Int J Cancer. 56, 46-51.

Wang, X., M. Rosol, S. Ge, D. Peterson, G. McNamara, H. Pollack, D. B. Kohn, M. D. Nelson and G. M. Crooks (2003). Dynamic tracking of human hematopoietic stem cell engraftment using in vivo bioluminescence imaging. Blood. 102, 3478-82.

Watson, S. A., D. Michaeli, T. M. Morris, P. Clarke, A. Varro, N. Griffin, A. Smith, T. Justin and J. D. Hardcastle (1999). Antibodies raised by gastrimmune inhibit the spontaneous metastasis of a human colorectal tumour, AP5LV. Eur J Cancer. 35, 1286-91.

FIGURE LEGENDS

Figure 1: Luminescence in two hESC clones following stable transfection with firefly luciferase.

Following transfection and selection of clones stably expressing firefly luciferase, $1x10^3$, $1x10^4$ or $1x10^5$ cells were plated out, treated with D-luciferin and their luminescence measured in the IVIS® X100 in comparison with the same numbers of a well-characterised stably transfected luminescent cell-line, PC3M. Error bars represent standard errors of the mean. Levels of luminescence in the two hESC clones was similar to that in the PC3Ms. One-way ANOVA, repeated measures test showed no significant difference between the 3 cell-lines ($p=0.38$) and the luminescence was proportional to the cell number.

Figure 2: Luminescence in differentiated and undifferentiated luciferase-expressing hESCs.

Two luciferase expressing hESC lines (hESC-luc7 and hESC-luc8) were differentiated as embryoid bodies for three weeks and disaggregated for luciferase assay (diff). Undifferentiated cells (at 3-5 passages higher) were trypsinsed and assayed (undiff). There was a significant increase in luminescence in both cells following differentiation (Student t-test, $p=0.006$ and $p<0.001$ for luc7 and luc8 respectively). Error bars represent standard errors of the mean.

Figure 3: Luminescence levels measured in chick embryos injected with hESC-Luc cells.

(A) HH Stage 16 embryo injected with 10^4 cells showed measurable luciferase signal *ex ovo*. (B-D) Embryos injected with 10^3 (B), 10^4 (C) and 10^5 (D) analysed *in ovo* showed measurable signal for the 2 higher doses tested, but not when 10^3 cells where injected (not detected, nd). (E) Graphical representation of bioluminescence values obtained for duplicate injections as in (C) and (D).

Figure 4: Real time imaging of tumour development in mice.

Luminescent hESC cells were injected into the intraperitoneal muscle wall (A) or the kidney capsule (B) and monitored over 75 days using luminescence imaging. Representative luminescence images of one mouse from each group are shown: brightfield images are overlaid with a pictorial representation of the intensity of photons emitted (blue = low light levels to red = high levels). The data for the 3 mice in each group that developed tumours are shown graphically.

Figure 5: Histological analysis of teratomas

Teratomas obtained from sacrificed mice were fixed, paraffin embedded, sectioned, and stained using Haematoxylin and Eosin. Mostly cystic structures were observed and an example of the histology of the cyst wall, composed of layers of dense extracellular matrix, is shown in A. Solid teratoma tissue was found containing a range of well-differentiated tissues including smooth muscle (B), gut-like secretory epithelium (C) and cartilage (D)

FIGURE 1

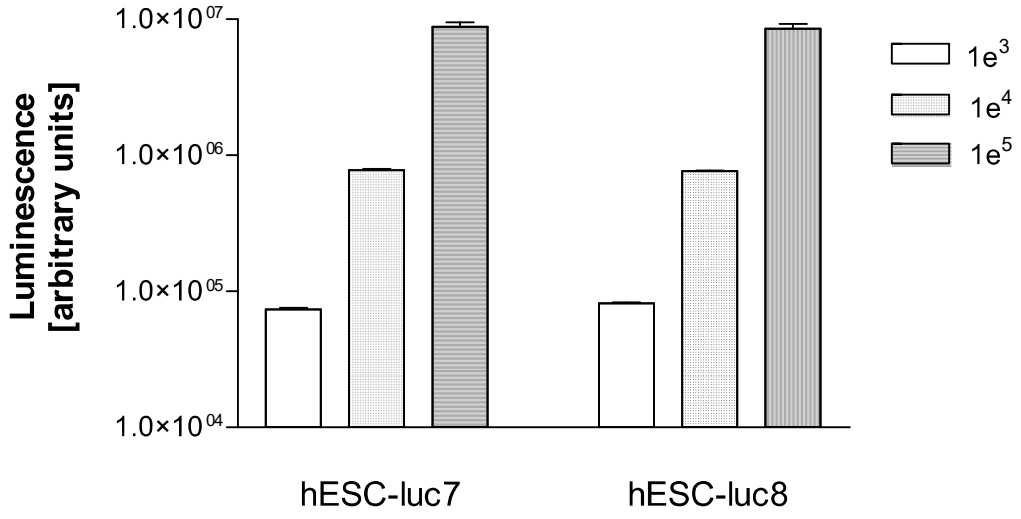
Luminescence [arbitrary units]
1.0×10^07
1.0×10^06
1.0×10^05
1.0×10^04
hESC-luc7
hESC-luc8
1e^3
1e^4
1e^5

FIGURE 2

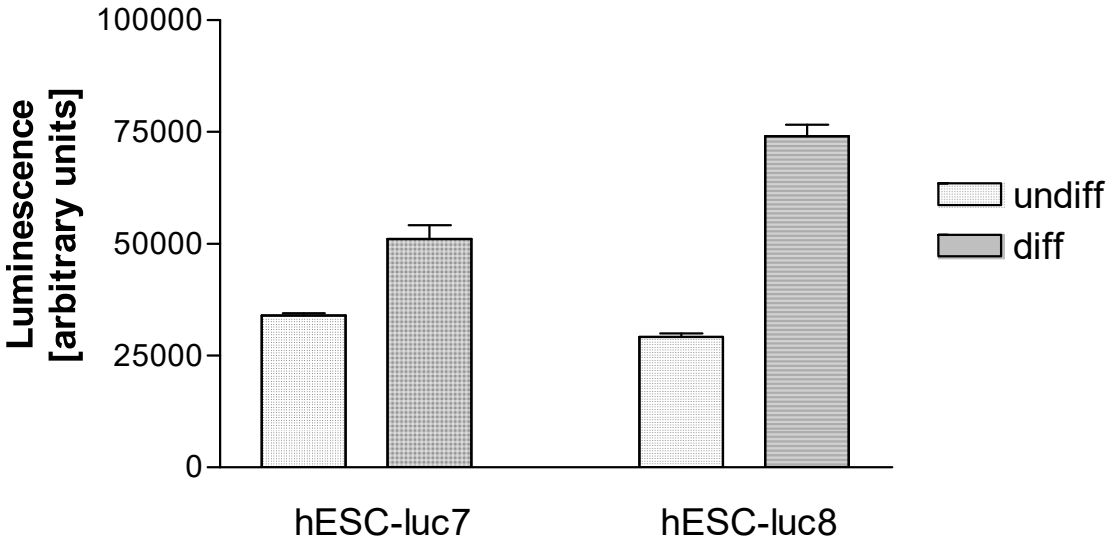
Luminescence [arbitrary units]
100000
75000
50000
25000
0
hESC-luc7
hESC-luc8
undiff
diff

FIGURE 3

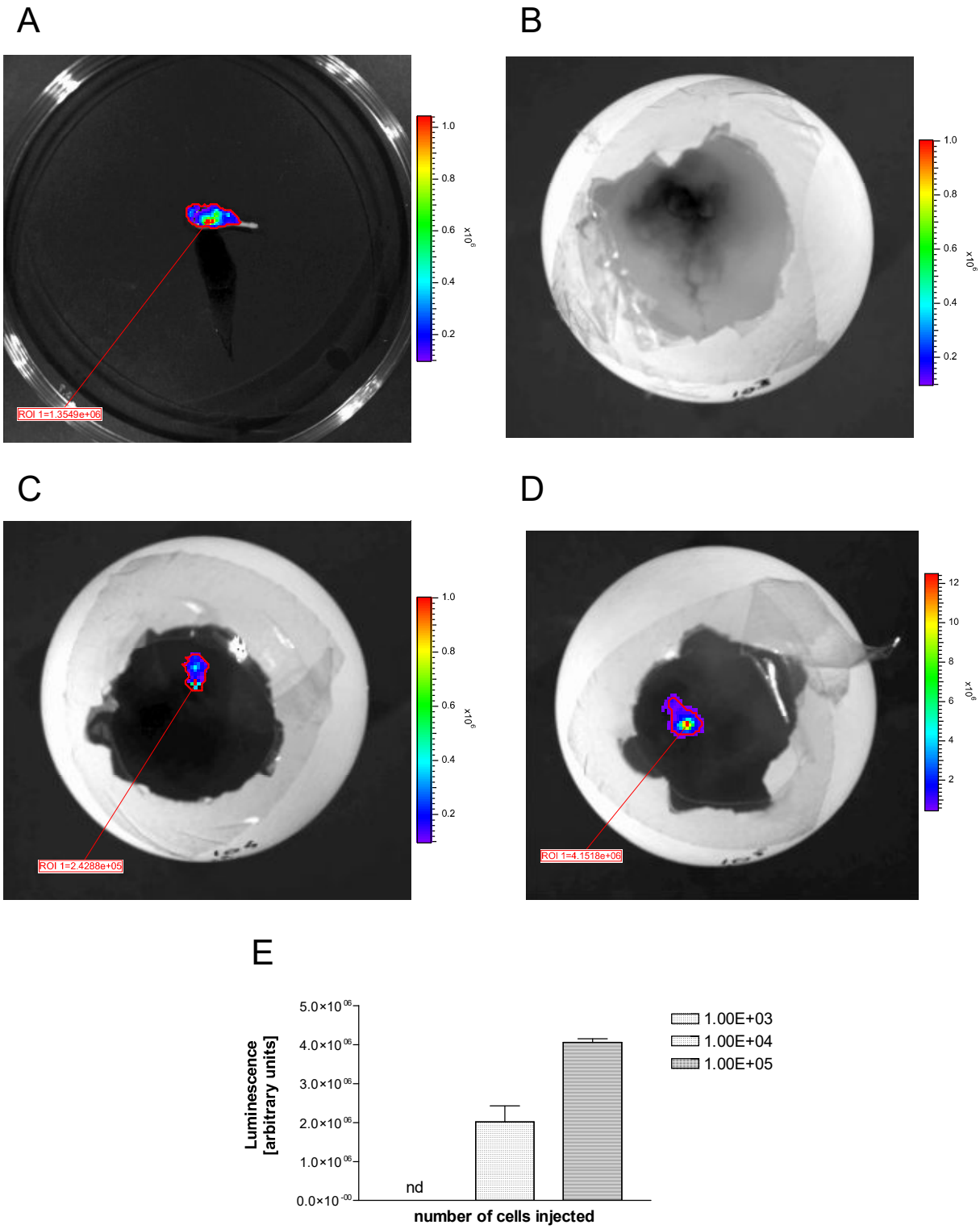
A
B
C
D
E
ROI 1=1.3549e+06
ROI 1=2.4288e+05
ROI 1=4.1518e+06
1.0
0.8
0.6
0.4
0.2
x10⁶
12
10
8
6
4
2
5.0×10⁰⁶
4.0×10⁰⁶
3.0×10⁰⁶
2.0×10⁰⁶
1.0×10⁰⁶
0.0×10⁻⁰⁰
Luminescence [arbitrary units]
nd
number of cells injected
1.00E+03
1.00E+04
1.00E+05

FIGURE 4

A

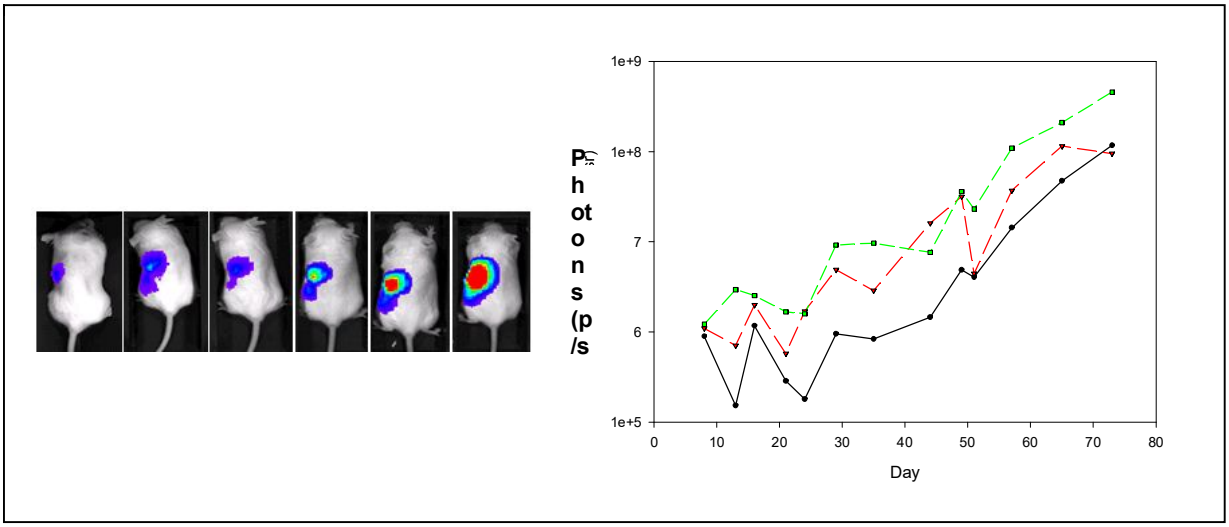
1e+9
1e+8
7
6
1e+5
Photons (p/s
0
10
20
30
40
50
60
70
80
Day

B

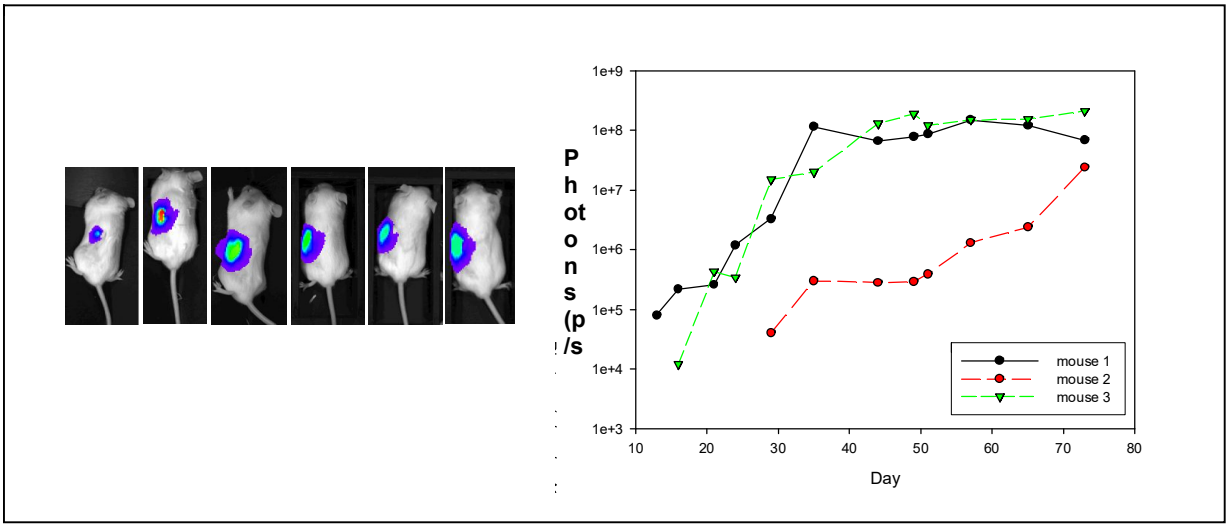
1e+9
1e+8
1e+7
1e+6
1e+5
1e+4
1e+3
Photons (p/s
10
20
30
40
50
60
70
80
Day
mouse 1
mouse 2
mouse 3

FIGURE 5